

## COMMUNICATION

[View Article Online](#)  
[View Journal](#) | [View Issue](#)



Cite this: *Nanoscale Adv.*, 2022, **4**, 3131

Received 17th May 2022

Accepted 18th June 2022

DOI: 10.1039/d2na00316c

[rsc.li/nanoscale-advances](http://rsc.li/nanoscale-advances)

## Highly active reduced graphene oxide supported Ni nanoparticles for C–S coupling reactions

Surjyakanta Rana,<sup>\*ab</sup> Jose J. Velázquez<sup>b</sup> and S. B. Jonnalagadda  <sup>\*a</sup>

Air-stable Ni nanoparticles (with particle size  $\sim 11$  nm) supported on reduced graphene oxide [ $\text{Ni}(0)@\text{RGO}$ ] was prepared by a simple and easy procedure. We previously described the Kumada–Corriu C–C cross-coupling reaction between iodo-arenes and Grignard reagents with  $\text{Ni}(0)\text{RGO}$  as a stable and efficient catalyst. This  $\text{Ni}(0)\text{RGO}$  catalyst gave an excellent yield (92%) and good recyclability (up to the 5<sup>th</sup> cycle). This communication confirms that the catalyst shows superior efficacy for the C–S coupling reaction, similar to that for the Kumada–Corriu C–C cross-coupling reaction. A catalytic experiment with the  $\text{Ni}(0)@\text{RGO}$  recycled material was also performed. HRTEM study of the reused material after the C–S coupling reaction confirmed the retention of the original (fresh) catalyst structure. It is reusable up to the 7<sup>th</sup> cycle without any activity loss.

Pursuing new organic frameworks and scaffolds has always been stimulating but remains challenging for researchers. Forming the C–C bond and the bond with heteroatoms with efficacy is fundamental to achieving the goal. Several cross-coupling reactions were designed using various transition metal catalysts.<sup>2–7</sup> Among the carbon–heteroatom bonds, the carbon–sulphur bond formation has received much attention due to the potential applications of various sulphur-containing heterocyclic molecules in the pharmaceutical or materials fields.<sup>8,9</sup> Different methods have been described for the C–S coupling reactions, *i.e.*, Teruaki *et al.* reported that  $\text{TiCl}_4$  and Zn formed 86% vinyl sulfide in the presence of dioxane–ammonia or pyridine in 10 h.<sup>10–12</sup> Cohen *et al.* stated that 93% vinyl phenyl sulfide formed with copper(i)-promoted thiophenoxy ionisation in solution in 72 h.<sup>13</sup> Akiyama *et al.* reported a 60% yield of 2-isopropyl-5-methyl-1-cyclohexenyl alkyl sulfides using aluminium chloride.<sup>14</sup> However, the traditional methods

require prolonged reactions, organic solvents, and potent reducing agents. Migita *et al.*, for the first time, reported a C–S coupling reaction for forming aryl halides and thiols employing  $\text{Pd}(\text{PPh}_3)_4$  as a homogeneous catalyst.<sup>15</sup> With the reusability potential, suitable heterogeneous catalysts can replace the homogeneous ones. Moreover, different metal-based heterogeneous catalysts containing expensive metals, such as Pd, Au, Ag *etc.*, were developed for coupling reactions during the last decade.<sup>16–24</sup> Some metal-based catalysts are highly efficient, giving high yields of the C–S coupling product at around 96%. The main disadvantage of these catalysts is the high cost of commercialisation. To overcome this drawback, few reports with low-cost metals, such as Ni-based catalysts for C–S coupling reactions, were reported in the past years.<sup>25,26</sup> Pal *et al.* described zirconia-supported NiO as a catalyst with low yield.<sup>27</sup> Thus, we used Ni nanoparticles supported by reduced graphene oxide (RGO) for the C–S coupling reaction to enhance the catalyst activity, as RGO possesses a high surface area and good electrical properties.<sup>28–32</sup> 2 : 1 ratio of graphite to sodium nitrate in the preparation was selected. This ratio increases the functional groups of the graphene oxide (GO) material. Therefore, this ratio raises the Ni nanoparticles binding capacity, *i.e.*, it is possible to load a high amount of Ni particles on the RGO surface, thus increasing the catalytic activity of carbon with a different heteroatom for the cross-coupling reaction.

This communication reports the catalytic activity of [ $\text{Ni}(0)@\text{RGO}$ ] for the C–S coupling reaction and the optimised reaction conditions. We also tested the C–S coupling reaction without any additives. The material [ $\text{Ni}(0)@\text{RGO}$ ] gave excellent yield and conversion.

To 2 mmol of  $\text{K}_2\text{CO}_3$ , one mmol of iodobenzene, 1.1 mmol of thiophenol, and 3 mL of dimethylformamide (DMF) were added, followed by 0.02 mg of catalyst. Further, the reaction mixture was stirred in a preheated oil bath at 90 °C for 3 h. After completion of the reaction, the solution was cooled to room temperature and diluted with ethyl acetate (5 mL). Then, the final products were analysed by gas chromatography.

<sup>a</sup>School of Chemistry & Physics, College of Agriculture, Engineering & Science, University of KwaZulu-Natal, Durban, South Africa. E-mail: [jonnalagaddas@ukzn.ac.za](mailto:jonnalagaddas@ukzn.ac.za); Fax: +27 31 260 3091; Tel: +27 31 260 7325/3090

<sup>b</sup>Department of Functional Materials, FunGlass – Centre for Functional and Surface Functionalized Glass, Alexander Dubček University of Trenčín, 911 50 Trenčín, Slovakia. E-mail: [surjyakanta.rana@tnuni.sk](mailto:surjyakanta.rana@tnuni.sk)



Detailed characterization studies, including X-ray diffraction study, Raman, scanning electron microscopy, transmission electron microscopy, and high resolution transmission electron microscopy with SAED patterns of Ni(0)@RGO, GO, and RGO materials, were reported by the authors in previous work.<sup>1</sup> Graphene oxide was converted entirely to reduced graphene oxide due to a reducing agent that transforms Ni(II) into Ni(0). XRD data confirmed the formation of Ni nanoparticles on the RGO surface. At the same time, the Raman study gave structural information about the bonding of carbon atoms. SEM and SEM/EDX provided information about the layered structure of graphene oxide and elemental composition (C, Ni, and O) of the Ni(0)@RGO material. The TEM and HRTEM showed that Ni nanoparticles possess an average particle size of 11 nm.

X-ray photoelectron spectroscopy (XPS) provided information about the binding energy of Ni 2p in the Ni(0)@RGO catalyst (Fig. 1). As shown in Fig. 1, the 852.8 eV and 872.9 eV binding energies represent Ni 2p<sub>3/2</sub> and Ni 2p<sub>1/2</sub>, respectively, which confirms the zero-oxidation state of the Ni catalyst.<sup>33</sup>

Although many studies on C–C, C–N, C–O, and C–S coupling reactions have been reported, most reactions demand various organic solvents, long reaction times, and expensive catalyst materials. Earlier, Rana *et al.* described a C–C coupling reaction using the Pd@RGO catalyst at 80 °C for 5 h which gave a 97% yield.<sup>22</sup> Later, Varadwaj *et al.* reported Pd substituted amine-functionalised clay for a C–C coupling reaction at 80 °C for 6 h with 97% and 96% biphenyl yields in Suzuki–Miyaura and Ullmann coupling, respectively.<sup>20</sup> So far, only a few articles on coupling reactions involving inexpensive metal catalysts have been published. Xu *et al.* reported that copper iodide (CuI) nanoparticles were active toward C–S coupling at 50 °C for 24 h offering a 93% yield.<sup>34</sup> Kashin *et al.* reported a 65% yield of the C–S coupling product using a nanostructured nickel thiolate catalyst in the presence of DMF solvent at 120 °C.<sup>35</sup> A 92% yield of the C–S coupling product using different substituents of diphenyl sulphides was reported by Sengupta *et al.*<sup>36</sup> They used the Ni/RGO catalyst at 100 °C for 3 h. The reactions in the literature above needed either a higher reaction time, high temperatures, or harmful solvents.

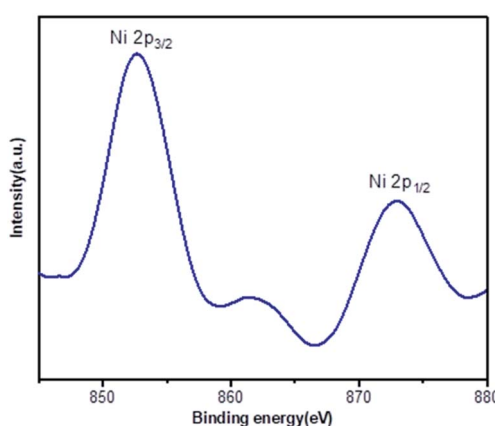


Fig. 1 XPS spectrum of the Ni 2p region of the Ni(0)@RGO material.

Table 1 Catalytic activity toward the C–S cross-coupling reaction<sup>a</sup>

Sl no.	Catalyst	Time (h)	Temp. (°C)	Yield (%)
1	Without catalyst	3	90	—
2	GO	3	90	13
3	Ni(0)RGO	3	90	94

<sup>a</sup> Iodobenzene (1 mmol), thiophenol (1.1 mmol), K<sub>2</sub>CO<sub>3</sub> (2 mmol) and DMF (3 mL) at 90 °C for 3 h.

Table 2 Optimisation of the C–S coupling reaction with different bases under similar conditions<sup>a</sup>

Sl no.	Base	Time (h)	Temp. (°C)	Yield (%)
1	K <sub>2</sub> CO <sub>3</sub>	3	90	94
2	K <sub>3</sub> PO <sub>4</sub>	3	90	87
3	KOH	3	90	85
4	Cs <sub>2</sub> CO <sub>3</sub>	3	90	91

<sup>a</sup> Iodobenzene (1 mmol), thiophenol (1.1 mmol) and DMF (3 mL) at 90 °C for 3 h.

In this communication, Ni(0) nanoparticles on reduced graphene oxide is reported as a catalyst toward a C–S coupling reaction under appropriate reaction conditions (lower reaction time and temperature). Aryl iodides with benzenethiol were examined in this coupling reaction with GO and Ni(0)@RGO materials as catalysts (Table 1). In the preliminary experiment, iodobenzene, thiophenol, K<sub>2</sub>CO<sub>3</sub> base, and DMF solvent at 90 °C for 3 h, were used for the C–S coupling reaction in the absence of a catalyst, and no products were formed. GO material was also used for the same coupling reaction under similar conditions, obtaining only a 13% yield. On the other hand, Ni(0)@RGO materials gave an excellent harvest (94%) with 100% substrate conversion under similar conditions.

The optimised reaction conditions were extended for a series of different bases. In particular, K<sub>3</sub>PO<sub>4</sub>, Cs<sub>2</sub>CO<sub>3</sub>, and KOH were

Table 3 Ni(0)@RGO catalysed C–S coupling reaction<sup>a</sup> between different aryl iodides and thiol substituents

Sl no.	Reactant-I	Reactant-II	Product	Yield (%)
1	X = I	X = SH	—	94
2	X = I, Y = OCH <sub>3</sub>	X = SH	Y = OCH <sub>3</sub>	61
3	X = I, Y = F	X = SH	Y = F	81
4	X = I, Y = Br	X = SH	Y = Br	89
5	X = I, Y = CH <sub>3</sub>	X = SH	Y = CH <sub>3</sub>	69
6	X = I, Y = NO <sub>2</sub>	X = SH	Y = NO <sub>2</sub>	91
7	X = Cl	X = SH	—	53
8	X = F	X = SH	—	31

<sup>a</sup> Different substituents of aryl iodide (1 mmol), thiophenol (1.1 mmol), K<sub>2</sub>CO<sub>3</sub> (2 mmol) and DMF (3 mL) at 90 °C for 3 h.



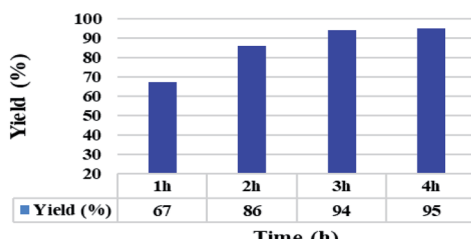


Fig. 2 Optimisation of reaction time using the Ni(0)@RGO material.

screened for the C–S coupling reaction with Ni(0)RGO materials and the results are shown in Table 2. The minimum obtained yield was 85% for the less expensive KOH base. Meanwhile, the maximum output of diphenyl sulphide was 94% for the  $K_2CO_3$  base.

The method's efficacy was assessed by conducting the C–S cross-coupling reactions using different substituents of aryl iodide with thiol under similar conditions in the presence of the Ni(0)@RGO catalyst (Table 3). The results illustrate that while the iodine substituent of the aryl reactant gave an excellent yield (94%), the fluoride substituent of the aryl reactant gave a lower yield (31%). The higher yield may be due to the weaker bond of C–I than that of C–F, as less energy will be required to break the C–I bond than that required for the C–F bond. On the other hand, both electron-donating and electron-withdrawing substituents of the aryl iodide reactant with thiol were also examined under similar conditions. The complex intermediate of the electron-withdrawing substituents ( $-NO_2$  and  $-Br$ ) of the aryl iodide reactant with the Ni catalyst favors the reductive elimination of the intermediate compared to that of the electron-donating substituents ( $-OCH_3$  and  $-CH_3$ ). Hence, the aryl iodides with the  $-Br$ – $-NO_2$  substituent give a better yield than those with the  $-OCH_3$ – $-CH_3$  substituent.

In addition, the reaction time for the C–S coupling reaction using the Ni(0)@RGO material was optimised, as shown in Fig. 2. It should be remarkable that only the reaction times of the scheme were changed, while the other parameters remained unaltered. Fig. 2 illustrates that the diphenyl sulphide yield increases with time up to 3 h. The product yield marginally varies with a further increase in the reaction time from 3 h to 4 h.

Temperature has a huge effect on the C–S coupling reaction. We studied the improvement of the reaction by varying the temperature parameter (Fig. 3). As can be seen from Fig. 3, the diphenyl sulphide yield increases with temperature up to 90 °C. The product yield marginally changes with a further increase in the reaction temperature from 90 to 100 °C.

We performed the same reaction with different solvents for optimisation and kept other parameters constant. Initially, we used green solvent water for the C–S coupling reaction at 90 °C for 3 h, which gave an 11% yield. A poorer result (9%) was observed with toluene as a solvent. DMF proved the best solvent for the C–S coupling reaction, offering superior yield.

A comparative summary of various reported materials for the C–S coupling reaction is tabulated in Table 4. An examination of

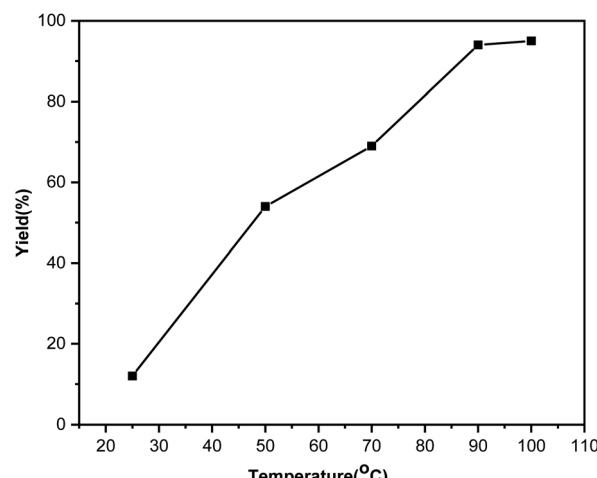


Fig. 3 Effect of different reaction temperatures on the C–S coupling reaction with the Ni(0)@RGO material.

Table 4 The effectiveness of the present work compared with reported results

Catalyst	Time (h)	Temp. (°C)	Yield (%)	Ref.
Cu-grafted furfural functionalized mesoporous material	8	100	85.2	37
Ni catalyst	3	100	92	36
CuI nanoparticles	24	50	93	34
Ni(0)RGO	3	90	94	Current work

the data shows that we achieved a higher yield in the current study with a shorter reaction time and lower temperature.

Fig. 4 illustrates the recycling experiments of the Ni(0)@RGO material for the C–S coupling reaction. In the recycling experiment, the catalyst was recovered from the reaction mixture by filtration, washed with ethyl acetate and water, and dried with acetone. As illustrated in Fig. 4, the Ni(0)@RGO material was active up to the 7<sup>th</sup> cycle.

Generally, transition metal (Pd, Ni, *etc.*) based catalysts are used for the C–S coupling reaction. The metal-based catalysts follow three mechanistic steps: oxidative addition, substitution, and reductive elimination. Further, the Ni catalyst is

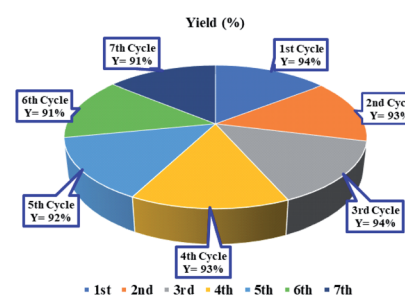
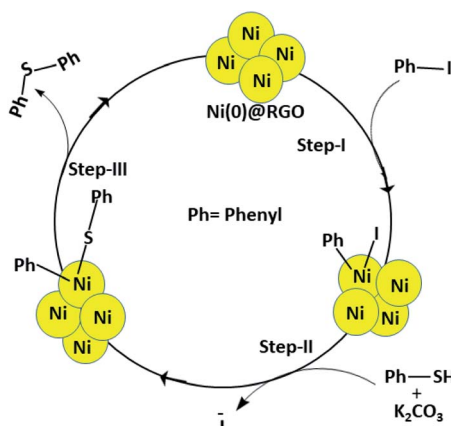


Fig. 4 Reusability result of the Ni(0)@RGO material for the C–S coupling reaction.





Scheme 1 Schematic presentation of the C–S coupling reaction.

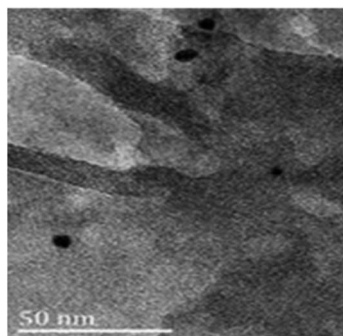


Fig. 5 HRTEM study of the Ni(0)@RGO material after the first run of the C–S coupling reaction.

inexpensive and readily available compared to other precious metal catalysts. Based on the experimental results, the C–S coupling reaction mechanism is proposed (Scheme 1).

Reused Ni(0)@RGO materials were characterised after the first run by HRTEM (Fig. 5). The average particle size of the Ni nanoparticles is 11 nm, which is very similar to that of the fresh Ni(0)@RGO material. This characterisation technique confirms the retention of the catalyst structure.

In conclusion, Ni nanoparticles on reduced graphene oxide display excellent catalytic activity for the C–S coupling reaction. A simple procedure was used to design the nanomaterial. XPS confirmed the zero-oxidation state of the Ni material. The Ni(0)@RGO materials gave a 94% yield of the diphenyl sulfide product in a shorter reaction time using less expensive reagents than those reported in the literature. The catalyst also displayed good stability in recycling tests.

## Conflicts of interest

There are no conflicts to declare.

## Author contributions

S. Rana – conceptualization, formal analysis, and original draft preparation. J. J. Velázquez – conceptualization and

investigation. S. B. Jonnalagadda – resources, methodology writing – review and editing, and supervision.

## Acknowledgements

The authors acknowledge the support received from the (i) School of Chemistry & Physics, University of KwaZulu-Natal, Durban, South Africa and (ii) Department of Functional Materials, FunGlass – Centre for Functional and Surface Functionalized Glass, Alexander Dubček University of Trenčín, Slovakia, for research facilities.

## Notes and references

- 1 S. Rana, G. B. B. Varadwaja and S. B. Jonnalagadda, *Nanoscale Adv.*, 2019, **1**, 1527–1530.
- 2 J. F. Hartwig, *Synlett*, 2006, 1283–1294.
- 3 G. Evano, N. Blanchard and M. Toymi, *Chem. Rev.*, 2008, **108**, 3054–3131.
- 4 S. Mallick, S. Rana and K. M. Parida, *Dalton Trans.*, 2011, **40**, 9169–9175.
- 5 S. Würtz and F. Glorius, *Acc. Chem. Res.*, 2008, **41**, 1523–1533.
- 6 A. Correa, O. García Mancheño and C. Bolm, *Chem. Soc. Rev.*, 2008, **37**, 1108–1117.
- 7 G. B. B. Varadwaj, S. Rana and K. M. Parida, *RSC Adv.*, 2013, **3**, 7570–7578.
- 8 C. M. Rayner, *Contemp. Org. Synth.*, 1996, **3**, 499–533.
- 9 J. A. Jordan-Hore, C. C. C. Johansson, M. Gulias, E. M. Beck and M. J. Gaunt, *J. Am. Chem. Soc.*, 2008, **130**, 16184–16186.
- 10 T. Yamamoto and Y. Sekine, *Can. J. Chem.*, 1984, **62**, 1544–1547.
- 11 M. Toshihiko, S. Tomiya, A. Yoriyoshi, S. Jun-ichi, K. Yasuki and K. Masanori, *Bull. Chem. Soc. Jpn.*, 1980, **53**, 1385–1389.
- 12 T. Mukaiyama, M. Shiono and T. Sato, *Chem. Lett.*, 1974, **3**, 37.
- 13 T. Cohen, G. Herman, J. R. Falck and A. J. Mura Jr, *J. Org. Chem.*, 1975, **40**(6), 812–813.
- 14 F. Akiyama, *Bull. Chem. Soc. Jpn.*, 1977, **50**, 936–938.
- 15 K. Masanori, O. Toshimi, T. Masahiro, S. Hiroshi and M. Toshihiko, *Bull. Chem. Soc. Jpn.*, 1985, **58**, 3657–3658.
- 16 S.-M. Lu and H. Alper, *J. Am. Chem. Soc.*, 2005, **127**(42), 14776–14784.
- 17 M. Opanasenko, P. Štěpnička and J. Čejka, *RSC Adv.*, 2014, **4**, 65137–65162.
- 18 A. Nijamudheen and A. Datta, *Chem.–Eur. J.*, 2020, **26**(7), 1442–1487.
- 19 S. Rana, G. B. B. Varadwaj and S. B. Jonnalagadda, *Nanomaterials*, 2021, **11**, 2260.
- 20 G. B. B. Varadwaj, S. Rana and K. Parida, *J. Phys. Chem. C*, 2014, **118**, 1640–1651.
- 21 S. Rana, S. Maddila, K. Yalagala and S. B. Jonnalagadda, *Appl. Catal. A*, 2015, **505**, 539–547.
- 22 S. Rana, G. B. B. Varadwaj and S. B. Jonnalagadda, *RSC Adv.*, 2019, **9**, 13332–13335.
- 23 N. Morita and N. Krause, *Angew. Chem.*, 2006, **118**, 1930–1933.



24 R. Das and D. Chakraborty, *Tetrahedron Lett.*, 2012, **53**, 7023–7027.

25 N. Ichiishi, C. A. Malapit, Ł. Woźniak and M. S. Sanford, *Org. Lett.*, 2018, **20**(1), 44–47.

26 G. T. Venkanna, H. D. Arman and Z. J. Tonzetich, *ACS Catal.*, 2014, **4**, 2941–2950.

27 N. Pal and A. Bhaumik, *Dalton Trans.*, 2012, **41**, 9161–9169.

28 A. K. Geim, *Science*, 2009, **324**, 1530–1534.

29 G. B. B. Varadwaj and V. O. Nyamori, *Nano Res.*, 2016, **9**, 3598–3621.

30 R. R. Nair, P. Blake, A. N. Grigorenko, K. S. Novoselov, T. J. Booth, T. Stauber, N. M. R. Peres and A. K. Geim, *Science*, 2008, **320**, 1308.

31 L. T. Qu, Y. Liu, J. B. Baek and L. Dai, *ACS Nano*, 2010, **4**, 1321–1326.

32 G. B. B. Varadwaj, O. A. Oyetade, S. Rana, B. S. Martincigh, S. B. Jonnalagadda and V. O. Nyamori, *ACS Appl. Mater. Interfaces*, 2017, **9**(20), 17290–17305.

33 *Handbook of X-Ray Photoelectron Spectroscopy*, Physical Electronics Division, Perkin-Elmer, 1979, vol. 55, p. 344.

34 X.-B. Xu, J. Liu, J.-J. Zhang, Y.-W. Wang and Y. Peng, *Org. Lett.*, 2013, **15**, 550–553.

35 A. S. Kashin, E. S. Degtyareva, D. B. Eremin and V. P. Ananikov, *Nat. Commun.*, 2018, **9**, 2936.

36 D. Sengupta, K. Bhowmik, G. De and B. Basu, *Beilstein J. Org. Chem.*, 2017, **13**, 1796–1806.

37 J. Mondal, A. Modak, A. Dutta and A. Bhaumik, *Dalton Trans.*, 2011, **40**, 5228–5235.

